

Changes in glial cell markers in recent and old demyelinated lesions in central pontine myelinolysis*

A. Gocht¹ and J. Löhler²

¹ Anatomisches Institut, Abteilung für Neuroanatomie, Universität Hamburg, Martinistrasse 52, D-2000 Hamburg 20, Federal Republic of Germany

² Heinrich-Pette-Institut für Experimentelle Virologie und Immunologie an der Universität Hamburg, D-2000 Hamburg 20, Federal Republic of Germany

Received July 26, 1989/Revised, accepted December 28, 1989

Summary. An immunohistochemical study was performed to compare glial reactions in recent and old lesions of central pontine myelinolysis (CPM). Regions of demyelination and destruction of oligodendrocytes, showed reduced immunoreactivity of myelin basic protein (MBP), myelin-associated glycoprotein (MAG), transferrin, and carbonic anhydrase C (CA C). In addition, labeling of glial fibrillary acidic protein (GFAP) and S-100 protein revealed distinct dystrophic alterations of the astroglia. Remarkably, immunolabeling of GFAP was drastically reduced in astrocytic cytoplasm within freshly demyelinated lesions. Immunostaining of vimentin revealed a differential intracytoplasmic decoration of hypertrophic and dystrophic astrocytes in recent and old CPM lesions. Immunolabeling of desmin failed to stain glial cells. Monoclonal antibodies against HNK-1 exhibited greatly increased immunoreactivity both of persisting oligodendrocytes and of reactive fibrillary astrocytes in old CPM foci. In freshly demyelinated lesions, enhanced immunoreactivity of the X-hapten (3-fucosyl-N-acetyllactosamine) was prominent in astroglia and oligodendrocytes. Simultaneously, reactive astrocytes revealed intracytoplasmic labeling of laminin. Quantitation of GFAP⁺ astroglia in fresh CPM and control cases revealed an increase in the number of astrocytes within the demyelinated foci and in the surrounding non-demyelinated pontine tissue of CPM cases. The occurrence of astroglial alterations in the demyelinated foci of CPM could be interpreted as “astroglial dystrophy” which may represent a pathogenic factor in CPM. Furthermore, it is possible that changes of the glial microenvironment may influence the astroglia to revert transiently back to an immature phenotype as indicated by the enhanced expression of the X-hapten and HNK-1, and the de novo synthesis of vimentin and laminin.

Key words: Central pontine myelinolysis – Demyelination – Astrocytes – Cell adhesion molecules – Immunohistochemistry

The term central pontine myelinolysis (CPM) was coined by Adams et al. [2] to designate a non-inflammatory demyelinating disease which mainly affects the middle portion of the pons. Later it was discovered that other regions of the CNS may be involved as well [15, 39, 57]. Obviously, the disease affects the oligodendroglia which leads to myelin breakdown [35] but for a long time astrocytic changes in CPM have also been described, such as hypertrophic astrogliosis [39, 57] and Alzheimer type II glia [16, 46]. More recently evidence has been accumulated suggesting an impaired astroglial function in the pathogenesis of this demyelinating disease [23, 36, 37]. This study was aimed at further characterizing the glial reactions in CPM. In this context our efforts focussed on two questions: (1) does the morphological spectrum of astroglial alterations support the concept of astrocytic dysfunction as an essential pathogenic event of CPM? and (2) are those molecules involved in the pathological process which were thought to function in cellular interaction or adhesion? To address these issues we performed immunocytochemical investigations in recent and old CPM lesions.

In this study antibodies, which are known to react with components of oligodendroglia and myelin {carbonic anhydrase C (CA C) [26, 27], transferrin [4], myelin basic protein (MBP) [22], myelin-associated glycoprotein (MAG) [51]}, as well as astrocytes {glial fibrillary acidic protein (GFAP) [30], S 100-protein [30]} in conventionally processed and paraffin-embedded brain tissue, were employed in ten autopsy cases of CPM, six of which contained fresh and four old lesions. Besides GFAP, the presence of vimentin and desmin, was investigated.

Growing evidence suggests that the functional plasticity and interdependence of glial cells is regulated by factors, such as cytokines and cell adhesion molecules,

* The Heinrich-Pette-Institut is financially supported by Freie und Hansestadt Hamburg and Bundesministerium für Jugend, Familie, Frauen und Gesundheit

Offprint requests to: A. Gocht (address see above)

Table 1. Clinical data in ten cases of central pontine myelinolysis (CPM)

Case no. ^a	Age (years)	Sex	Alcoholism	Electrolyte disturbances	Liver diseases ^b	Hypotension
1	36	f	+	+	+	+
2	50	m	+	+	+	+
3	42	f	+	+	+	+
4	46	m	+	+	+	+
5	63	m	+	+	+	+
6	50	f	+	+	+	+
7	50	m	+	+	+	+
8	35	m	+	+	+	+
9	42	f	+	+	+	+
10	45	m	+	+	+	+

^a No. 1–6: fresh lesions; No. 7–10: old lesions

^b Cirrhosis or fatty changes
Na \downarrow ↑: Rapid rise in serum sodium

but little is known about their role in pathological processes. Therefore, we have included in our study the investigation of HNK-1 and 3-fucosyl-*N*-acetylactosamin (X-determinant) reactivity in CPM. These molecules are associated with cell interaction or cell adhesion functions of the CNS ([34], reviewed in [44]). Additionally, the extracellular matrix glycoprotein laminin, normally a constituent of basal laminae [52], was examined in CPM lesions.

In all CPM cases astroglial alterations were found, most of which were of a degenerative nature. Therefore, we decided to quantitate GFAP⁺ astrocytes in seven cases with recent well-circumscribed CPM foci.

Materials and methods

Of ten autopsy cases with CPM (Table 1) horizontal brain stem slices from the upper and mid-pons level were dissected after fixation in 4% formalin. Normal brain tissue was taken from a 31-year-old man who died from injury of the femoral artery and trachea, and a 54-year-old woman who died from acute cardiac failure.

Tissue blocks were embedded in Histosec (Merck, Darmstadt, FRG) and cut at 10–12 μ m. Sections were stained with cresyl violet, hematoxylin-eosin, Heidenhain's, Klüver-Barrera's, Holzer's stain, and silver impregnated by Bodian's technique. Frozen material was used for Sudan III reaction.

Immunocytochemistry

The following antisera and conjugates were obtained from commercial sources: rabbit anti-GFAP antiserum (Dakopatts, Hamburg, FRG), rabbit anti-human MBP antiserum (Dakopatts), rabbit anti-human transferrin antiserum (Dakopatts), affinity-purified rabbit anti-laminin antibodies and antiserum (Polysciences Inc., Warrington, Pa and E-Y Laboratories, San Mateo, Calif, respectively) biotinylated goat anti-mouse IgM and IgG (Sigma, Deisenhofen, FRG), peroxidase-conjugated and alkaline phosphatase-conjugated streptavidin-biotin complex (Dakopatts).

Rabbit anti-MAG antibodies which had been purified by affinity chromatography were a generous gift from F. Kirchhoff (Neurobiologie der Universität Heidelberg, Heidelberg, FRG) [3], and rabbit anti-human CA C antiserum was kindly donated by T. Kumpulainen (Department of Neurosurgery, University Central Hospital of Tampere, Tampere, Finland) [26, 27]. Sheep anti-rabbit immunoglobulin antiserum and rabbit peroxidase anti-peroxidase

(PAP) complex were produced and generously supplied by G. Rutter of the Heinrich-Pette-Institut.

Monoclonal mouse anti-vimentin and anti-desmin were purchased from Dakopatts. Anti-X-hapten and anti-HNK-1 monoclonal antibodies were used as hybridoma culture supernatants of the MMA clone [19] and HNK-1 clone [1] which were obtained from the American Type Culture Collection (Rockville, Md) and kept under standard hybridoma culture conditions in our laboratory.

For the immunocytochemical demonstration of the various antigens in routinely processed paraffin-embedded tissue either the PAP method [50] or the avidin-biotin-peroxidase complex (ABC) technique [20] were employed. Briefly, deparaffinized and rehydrated sections were digested for 6 min with 0.01% protease type XXIV (Sigma) in 0.05 M Tris-buffered saline (pH 7.6), or treated for 9 min with 3 M urea in 0.05 M Tris-buffered saline, before overnight incubation with appropriately diluted primary antibodies or antisera at 4°C was performed. For HNK-1 immunolabeling deparaffinized sections were delipidized in chloroform for 24 h prior to protease treatment [40]. The next steps were incubation with bridging or biotinylated second antibodies, followed by the PAP or the peroxidase- or alkaline phosphatase-conjugated strept-ABC. Alkaline phosphatase was disclosed using AS-MX-phosphate (Sigma) as substrate and Fast-Blue BB salt (Serva, Heidelberg, FRG) as coupling reagent [33]. To block endogenous alkaline phosphatase activity, levamisole (Sigma) was added to the substrate. The peroxidase was developed by the method of Graham and Karnovsky [18] using 3,3'-diaminobenzidine tetrahydrochloride (Sigma) as co-substrate.

When immunolabeling resulted in a weak yet specific signal (e.g., laminin), a silver intensification of the peroxidase reaction product was employed which avoids the reaction with agyrophilic tissue elements [13].

Specificity controls for the different immunohistochemical reactions were obtained either by incubating with nonimmune serum instead of the primary antiserum, or by omitting the primary antiserum. As controls for monoclonal antibodies an irrelevant mouse monoclonal antibody of the same immunoglobulin isotype was used.

Quantitative analysis of astrocytes

For quantitation of GFAP⁺ astrocytes, seven cases (a–g in Table 3; five males and two females with a mean age of 49.3 years) with well-circumscribed single CPM foci of recent origin were selected. Normal controls (h–k in Table 3) contained two females and two males (mean age 42.8 years) without any pathological changes of the brain and spinal cord. For both, CPM and control cases, the pons was horizontally cut at the level of the locus ceruleus. Immunostaining of GFAP was performed as described above. Cases

with old CPM foci were excluded from quantitation because reactive fibrillary astrocytes sometimes fail to stain for GFAP, presumably due to polymerization of the glial filaments [8, 10]. In CPM cases the centrally located foci were delineated according to infiltration of macrophages. Additionally, the margin of demyelination was verified in adjacent sections stained with Heidenhain's stain. The foci were marked with a felt-pen on the cover slip. Unaffected tissue at the basis pontis of the same section was chosen as intraindividual control area. Together the encircled control areas were approximately of the same dimensions as the CPM foci.

In control cases a centrally located area was delineated which corresponded in its size to that of the demyelinated foci. Bi-laterally situated areas of basis pontis were encircled as well.

For quantitation a disc, engraved with a frame which measured 0.2025 mm^2 at 250 times magnification, was inserted into one eyepiece of a standard microscope (Zeiss, Oberkochen, FRG.) The number of immunoreactive nucleated glial cells within the marked areas was counted at a magnification of $\times 250$. Counts were performed as systematic sampling by spacing the sample units according to a chessboard lattice which was then randomly applied to the areas to be measured [55]. The counts were repeated four times and expressed as number of cells per mm^2 area.

Statistical analysis included the Wilcoxon test for evaluation of intraindividual differences in paired observations (central vs. lateral areas within each group). The Mann-Whitney test was used for comparison of interindividual differences (CPM cases vs. controls). The calculated *P* values have to be interpreted as descriptive figures because no alpha-correction has been performed to correct the multiple test situation.

Results

Clinical data

Clinical findings are summarized in Table 1. In all ten cases chronic alcoholism was present. Other predominating disorders were liver cirrhosis, fatty liver changes and electrolyte disturbances. In one case a rapid rise in serum sodium was recorded.

Histopathological observations

In six cases, lesions of recent origin were found. These were characterized by infiltration of abundant lipid-laden

macrophages, and the absence of reactive fibrillary gliosis. Microcavitation occurred only in a mild form or was absent. Neuronal perikarya and axons were unchanged. Five cases with fresh alterations showed hyaline rod-like to club-shaped bodies with about 5–10 μm in diameter which resembled Rosenthal fibers. In three of these cases multinucleated gemistocytes were found within the lesions. Based on tissue reaction and the duration of neurological symptoms, these fresh lesions were estimated to be approximately 4 weeks old.

Four cases revealed old lesions with cavitations, few macrophages, and marked fibrillary gliosis. Hyaline rod- and club-shaped bodies as well as multinucleated astrocytes could be detected in two of these cases. Throughout the lesions nerve cells and axons were well-preserved. Considering the onset of the neurological manifestation and histological features, one would suppose that these cavitating lesions were several months old.

In contrast to previous reports [16, 46], Alzheimer type II glia could not be detected either within the myelinolytic lesions, or in other locations.

Immunohistochemical findings

The immunohistochemical findings in fresh and old CPM foci are summarized in Table 2.

GFAP, S-100 protein, Vimentin, and Desmin. Immunostaining of GFAP revealed distinct astroglial alterations dependent on the histological age of the CPM lesions.

Freshly demyelinated lesions were surrounded by numerous strongly GFAP⁺ hypertrophic astrocytes (Fig. 1a). In the center of recent foci, abundant hypertrophic reactive astrocytes were detectable which were only faintly labeled for GFAP (Fig. 1b). Many of these gemistocytes bore intracytoplasmic vacuoles. A portion of the GFAP⁺ cells showed shrunken perikarya with sparse processes and lobulated or pyknotic nuclei (Fig. 1c). Probably these cells represent degenerating astrocytes. Occasionally, macrophages were seen with weakly GFAP⁺ granular material in their cytoplasm. In

Table 2. Immunohistochemical findings in ten cases of CPM^a

Antigen	Fresh CPM foci (<i>n</i> = 6)				Old CPM foci (<i>n</i> = 4)			
	Astro	Oligo	Myelin	Macroph	Astro	Oligo	Myelin	Macroph
GFAP, S-100 P	+ (central) +++ (marginal)	0	0	+	+ (central) +++ (marginal)	0	0	+
Vimentin	+	0	0	0	+	0	0	0
MBP	0	0	+	+	0	0	0	0
MAG	0	0	+	+	0	0	0	0
Transferrin	++	0	0	++	+	0	0	+
CA C	0	++	+	+	0	++	+	+
X-Determinant	+++	+++	0	+	+	+	0	+
HNK-1	0	++	++	0	+++	+++	0	0
Laminin	+	0	0	0	0	0	0	0

^a 0: No; +: weak; ++: medium; +++: intensive immunostaining; central: at the center of the lesion; marginal: at the edge of the myelinolytic focus

Astro: astroglia; Oligo: oligodendroglia (perikarya); Macroph: macrophages; GFAP: glial fibrillary acidic protein; S-100 P: S-100 protein; MBP: myelin basic protein; MAG: myelin-associated glycoprotein; CA C: carbonic anhydrase C

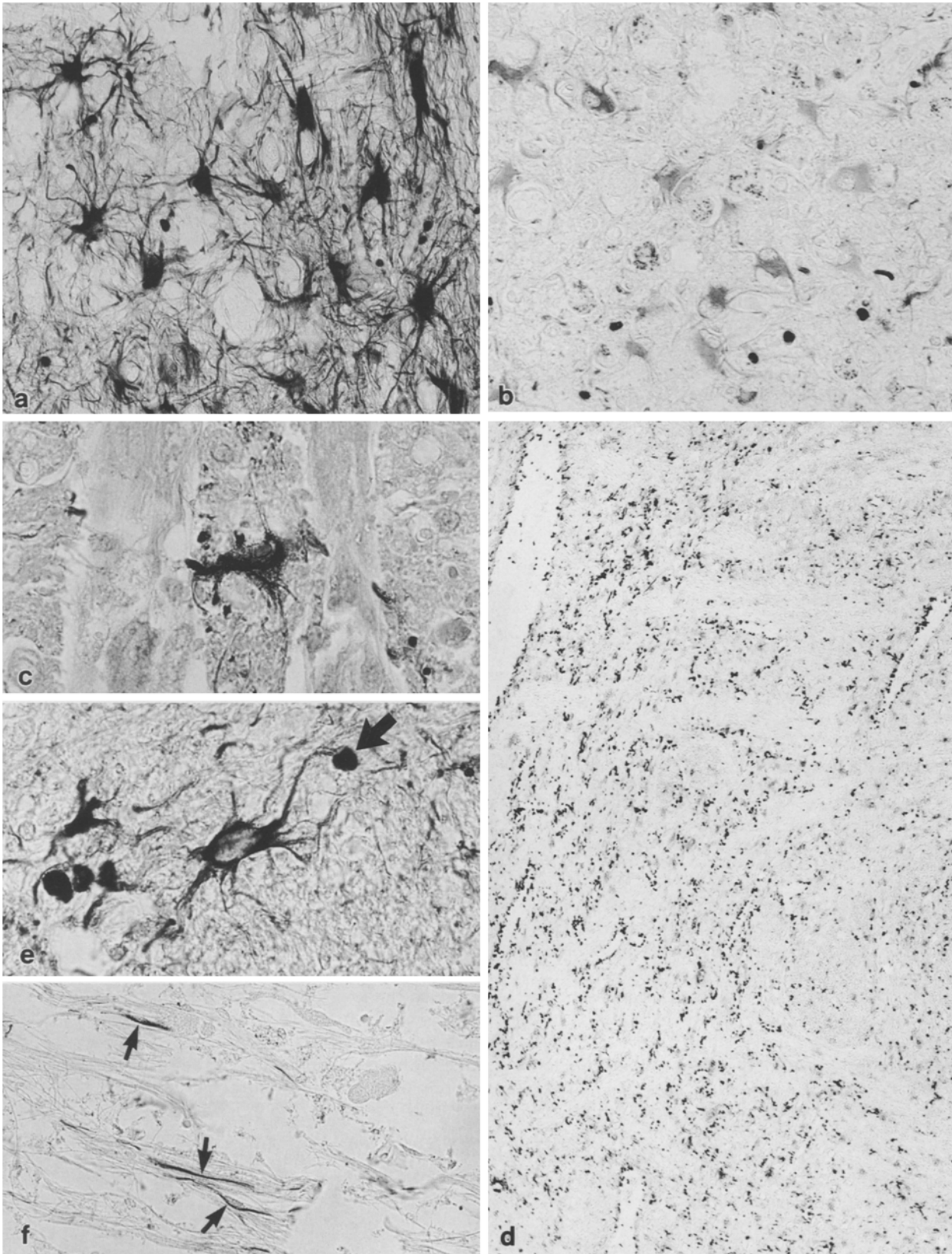


Fig. 1 a–f. Immunostaining of glial fibrillary acidic protein (GFAP) in recent (**a–e**) and old (**f**) central pontine myelinolysis (CPM) lesions. **a** Case 6. Intensely decorated hypertrophic astrocytes at the margin of the lesion, $\times 260$. **b** Case 6. Faintly labeled hypertrophic astrocytes within the center of the lesion, $\times 330$. **c** Case 2. A degenerating astrocyte with condensed nucleus and granular cytoplasm (slight counterstaining with hemalum), $\times 840$. **d** Case 1.

Low-power view of an area with numerous GFAP⁺ club- and rod-shaped bodies which resemble Rosenthal fibers, $\times 65$. **e** Case 1. Higher magnification of **d**. An astrocyte shows a process with a strongly GFAP⁺ club-like extension (*arrow*), $\times 710$. **f** Case 10. An old gliotic lesion discloses reactive fibrillary astrocytes with delicate elongated processes which are only faintly stained with anti-GFAP (*arrows*), $\times 320$

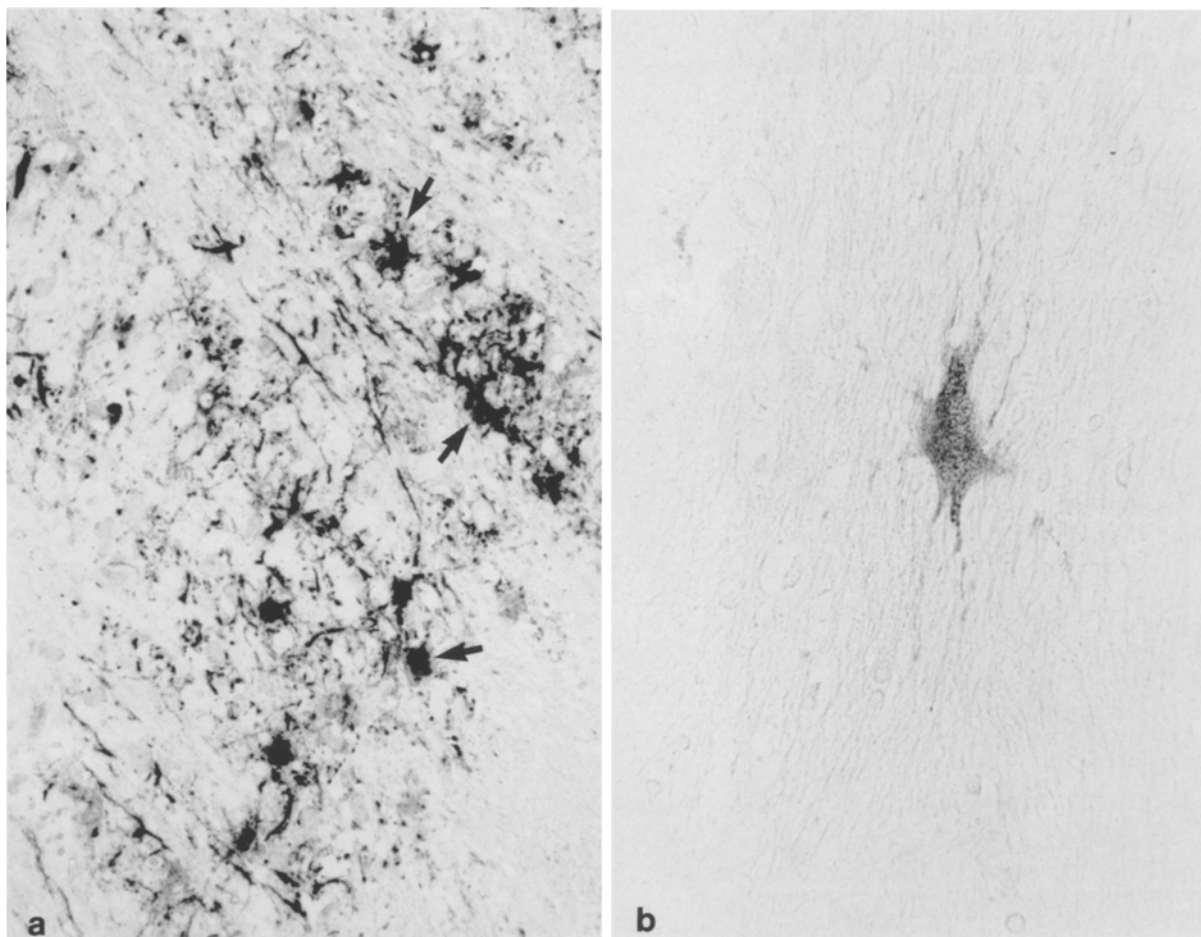


Fig. 2a, b. Immunolabeling of vimentin in a fresh (**a**) and old (**b**) CPM lesion. **a** Case 4. Within the lesion numerous vimentin⁺ astrocytic processes and some vimentin⁺ astrocytes, which exhibit degenerative changes, are visible. *Arrows* indicate astrocytes with intracytoplasmic labeling. For better visualization of the weak, yet

specific labeling signal a silver amplification method was used as described in Materials and methods, $\times 180$. **b** Case 10. Vimentin⁺ hypertrophic astrocyte at the margin of the lesion, no silver amplification, $\times 450$

five cases, the demyelinated lesions revealed abundant, strongly GFAP⁺ rod- and club-shaped structures (5–10 μm in diameter) which accumulated around blood vessels (Fig. 1d). These bodies could be clearly assigned to astrocytic processes (Fig. 1e) and resembled Rosenthal fibers as was mentioned above. In two of these cases GFAP⁺ club-like bodies and gemistocytes were also found outside the lesion within the unsevered myelinated pontine tissue.

Old foci revealed dense gliosis consisting of fibrillary astrocytes that exhibited extremely faint immunolabeling of GFAP (Fig. 1f). At the margin of these gliotic lesions intensively stained hypertrophic astrocytes could be seen that resembled those of recent lesions. Again degenerating astrocytes and GFAP⁺ macrophages could be observed. Strongly GFAP⁺ rod- and club-shaped bodies were also seen in two cases with old lesions. In one of these cases, the area with these structures extended to the unaffected peripheral tissue. The results of S-100 protein labeling were identical to those of GFAP.

In normal pontine tissue vimentin immunoreactivity was confined to leptomeninges and blood vessels. However, within recent CPM foci many astrocytes which were

identified as degenerating or, less frequently, as hypertrophic forms proved to stain with anti-vimentin (Fig. 2a). Astroglial cells within non-demyelinated peripheral pontine tissue lacked vimentin immunoreactivity. In the cases with old CPM lesions only individual cells of the hypertrophic astrocytes which encircled the demyelinated areas were vimentin⁺ (Fig. 2b). At the center of the demyelinated foci as well as in the unaffected portions of the pons astrocytes were negative for vimentin.

In normal pontine tissue immunostaining of desmin was restricted to smooth muscle cells in blood vessels. The same held true for the CPM cases.

MBP, MAG, transferrin, and CA C. In lesions of recent origin, myelin sheaths were largely negative for MBP except for a few small bundles of faintly labeled myelin fibers (Fig. 3a). Many macrophages contained weakly stained, MBP⁺ material in their cytoplasm. Virtually no MBP immunostaining was detectable within old foci (Fig. 3b). A pattern of immunoreactivity identical to that of MBP was obtained after application of anti-MAG antiserum.

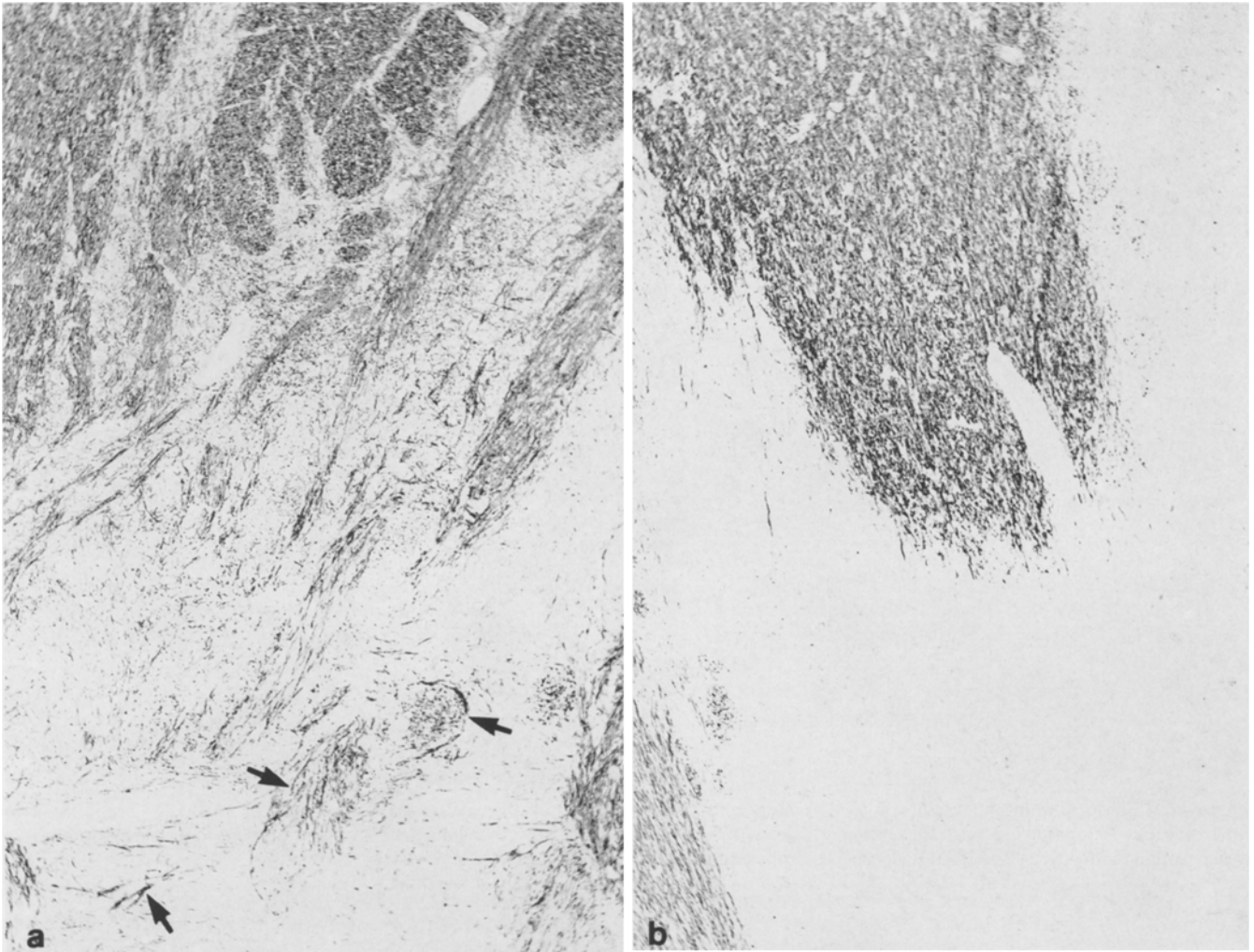


Fig. 3 a, b. Immunostaining of myelin basic protein (MBP) in a fresh (a) and an old (b) CPM focus. **a** Case 7. Within the lesion (lower part of the micrograph) MBP staining is markedly decreased; however, some preserved myelin fibers are still present (arrows), $\times 50$.

b Case 8. Normal staining intensity of MBP is present in unaffected pontine tissue. Within the demyelinated area no immunoreactivity is visible (lower part). Notice the sharp demarcation of demyelinated and unaffected areas, $\times 50$

Transferrin which is regarded by some authors as a marker protein for oligodendrocytes [4] could not be traced in oligodendroglial cells of fresh or old foci of demyelination, although persisting oligodendrocytes could be identified immunohistologically by use of CA C (see below). However, the oligodendroglia of the adjacent non-demyelinated pontine tissue could be readily tagged by anti-transferrin antiserum (Fig. 4a). As was to be expected, macrophages also stained positively with anti-transferrin (Fig. 4b). Unexpected, however, was the positivity of hypertrophic astrocytes in freshly demyelinated foci (Fig. 4c) and at the margins of old lesions. Fibrillary astrocytes that reside inside the old foci were only faintly labeled with anti-transferrin. To our knowledge, transferrin labeling in astrocytes has not been reported so far. It remains to be verified whether transferrin is constitutively expressed in activated astrocytes or if the transferrin labeling is the result of transferrin uptake by astroglial cells.

Immunocytochemical visualization of CA C which, according to Kumpulainen and co-workers [26, 27], is a

reliable marker of oligodendrocytes and myelin revealed a marked reduction in the numbers of oligodendrocytes within the lesions, similar to the results obtained with anti-transferrin. However, in recent as well as old foci scattered, properly stained oligodendrocytes were always visible (Fig. 5) and, on closer inspection, presented cytoplasmic swelling. It should be stressed that CA C immunolabeling was restricted to the perikarya of oligodendrocytes but was absent within adjacent myelin sheaths.

X-determinant and HNK-1. Since increasing evidence is presented in the literature that neural adhesion molecules, such as Le^x and HNK-1, play an important role in the functional organization of the CNS, we were stimulated to study the expression of these carbohydrate structures in CPM foci. In normal pontine tissue of controls, antibodies to the X-determinant revealed surface labeling of astrocytes and intracytoplasmic staining of oligodendrocytes (Fig. 6a) in accordance with previous reports [31, 34]. In addition, finely granular labeling of the

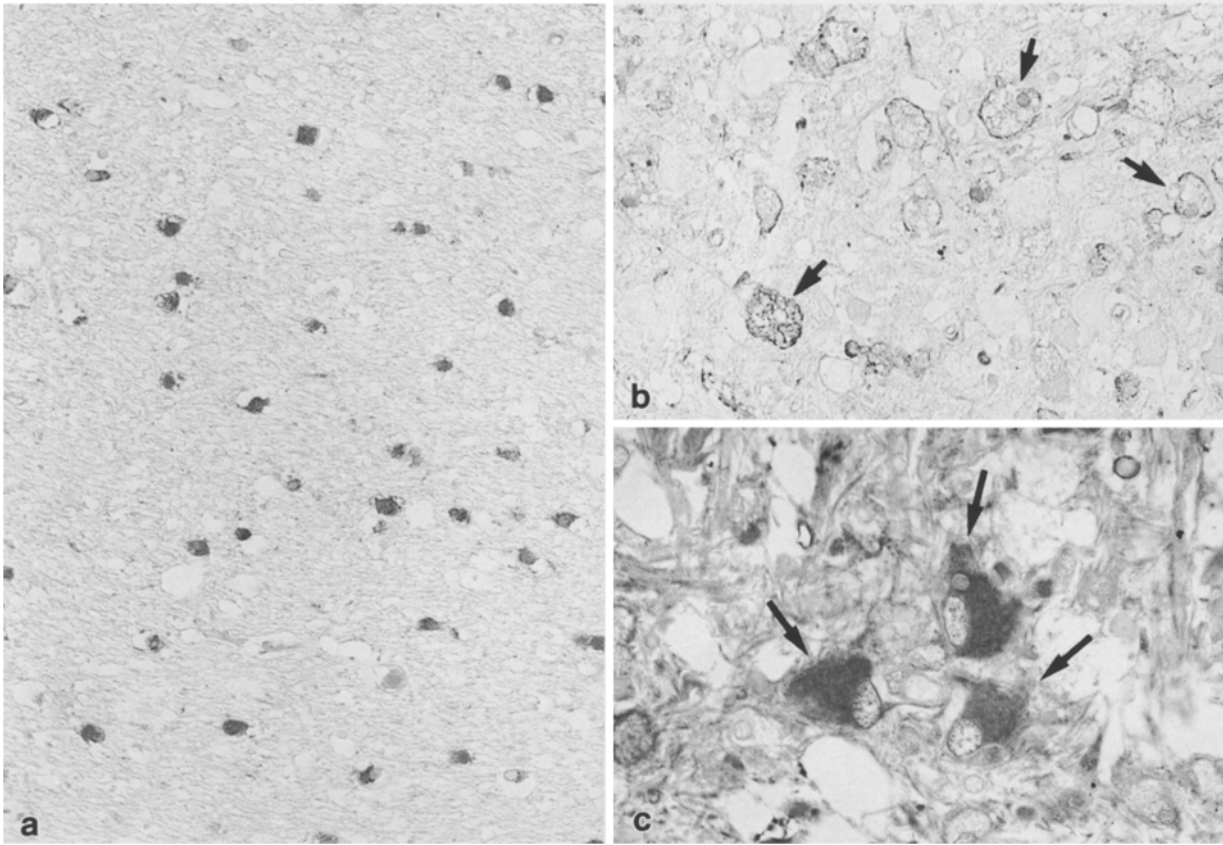


Fig. 4a–c. Immunostaining of transferrin in two cases with fresh CPM. **a** Case 3. Unaffected part of pontine tissue with several labeled oligodendrocytes, $\times 315$. **b** Case 3. Labeled foamy

macrophages within the lesion (*arrows*), $\times 315$. **c** Case 6. Several labeled hypertrophic astrocytes at the margin of a fresh lesion (*arrows*), $\times 460$

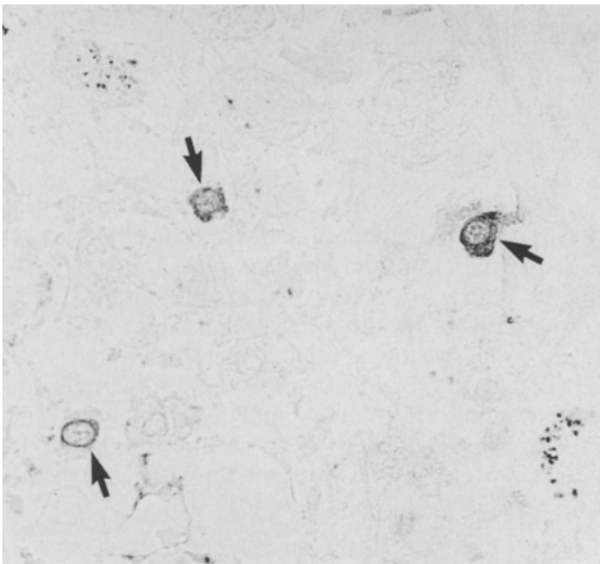


Fig. 5. Immunostaining of carbonic anhydrase C in a case of fresh CPM (case 6). A few labeled oligodendrocytes within the demyelinated tissue (*arrows*), $\times 700$

neuropil was seen. Myelin fibers were not immunostained. Freshly demyelinated CPM lesions disclosed scattered patches with greatly enhanced anti-X-determinant antibody binding. Most of the increased X-hapten immunoreactivity was due to strong cell surface

antibody decoration of astrocytes (Fig. 6b), but preserved oligodendrocytes also exhibited strong antibody binding, as did the neuropil. In the latter case, the reaction product could not be attributed to defined cellular structures. It is noteworthy that enhanced immunoreactivity was not only found with hypertrophic astrocytes but also with severely dystrophic astrocytes displaying shrunken perikarya and condensed nuclei. In older lesions X-determinant immunostaining was ubiquitously reduced. Numerous reactive fibrillary astrocytes as well as a few persisting oligodendrocytes were only faintly tagged (Fig. 6c).

Antibodies to the HNK-1 epitope showed a reverse staining pattern of recent and old lesions compared to the X-determinant. In fresh CPM lesions persisting oligodendrocytes and myelin fibers disclosed an intermediate staining intensity of HNK-1 (Fig. 7a), comparable to normal control tissue. On the other hand, in older lesions HNK-1 labeling was greatly enhanced within the cytoplasm of persisting oligodendrocytes and within the perikarya of reactive fibrillary astrocytes. Additionally, strong expression of HNK-1 was observed on remnants of myelin sheaths at the margin of old CPM foci (Fig. 7b).

Laminin. Laminin, which is a constituent of basal laminae [52], is not normally found in the cytoplasm of neuronal or glial cells of adult mammals, other than in the olfactory bulb of rats where laminin is continuously expressed by

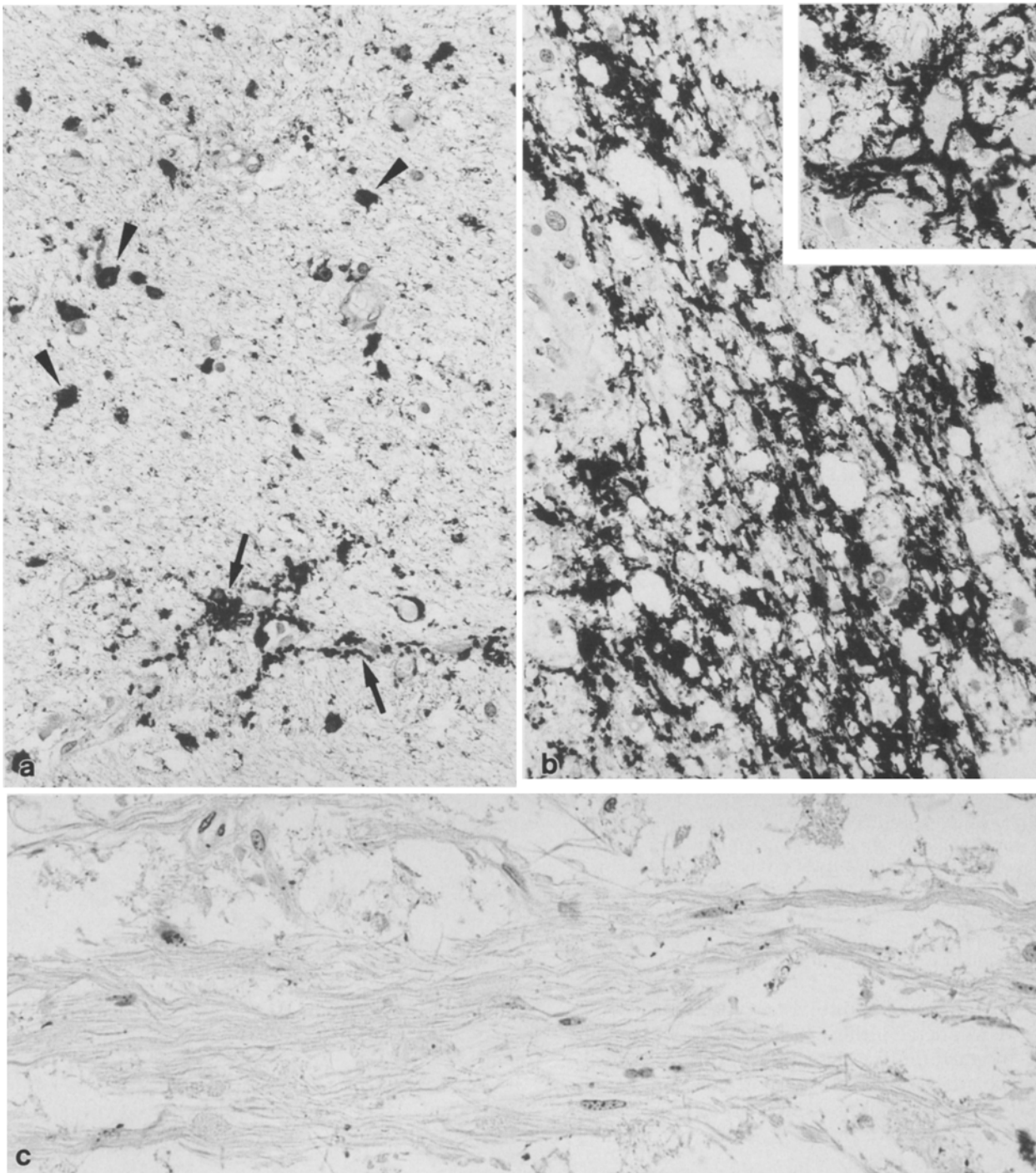


Fig. 6a–c. Immunostaining of X-determinant in control pontine tissue (**a**), in a recent (**b**), and an old (**c**) CPM lesion (slight counterstaining with hemalum). **a** Normal pontine tissue shows intracytoplasmic tagging of oligodendrocytes (*arrowheads*) and fine granular decoration of astrocytic perikarya and processes (*arrows*), $\times 365$. **b** Case 3. Within the freshly demyelinated tissue strong

immunoreactivity is predominantly associated with reactive astrocytes. The inset depicts a hypertrophic astrocyte with strong immunoreactivity at the surface of the perikaryon and the processes, $\times 365$. **c** Case 10. The micrograph displays an old lesion with fibrillary gliosis. Virtually no antibody decoration is visible, $\times 490$

astrocytes [28]. In fresh CPM foci, however, occasionally weakly stained laminin⁺ reactive astrocytes could be detected (Fig. 8). The laminin reactivity of astrocytes was obtained by use of two different antisera; the appropriate controls led to negative results (see Materials and

methods). The laminin staining of astrocytes became more prominent when silver enhancement of the peroxidase reaction product was performed. Laminin labeling of vascular basal laminae was not changed in fresh or old CPM foci.

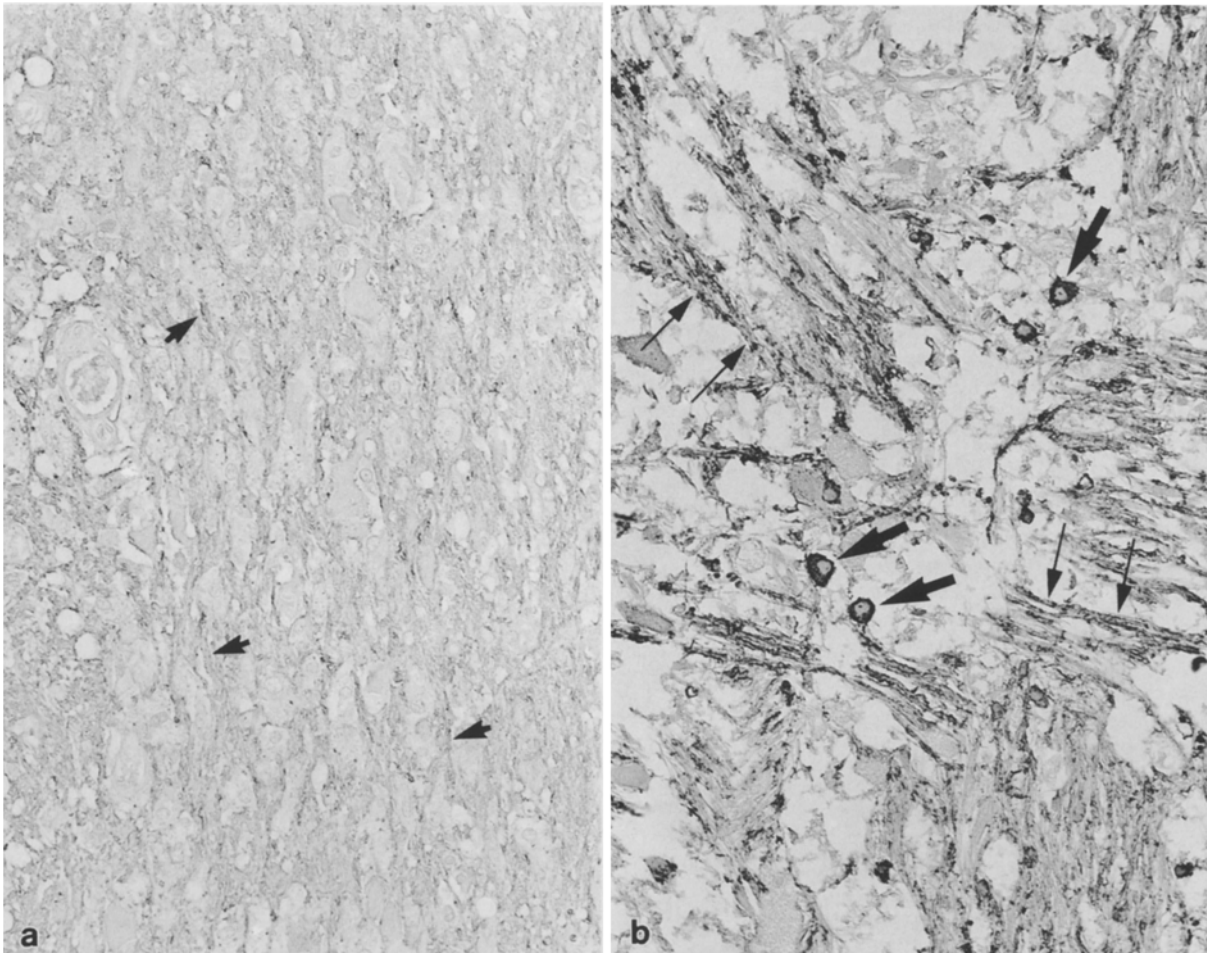


Fig. 7a, b. Immunostaining of HNK-1 in a fresh (**a**) and an old (**b**) CPM focus (slight counterstaining with hemalum). **a** Case 2. Within the recent lesion the staining intensity of myelin sheaths (*arrows*) is comparable to that in normal pontine tissue, $\times 300$. **b** Case 8. The

micrograph depicts the margin of an old lesion. A strong labeling of swollen oligodendrocytes (*thick arrows*) and of remnants of myelin sheaths (*thin arrows*) can be recognized, $\times 300$

Quantitative analysis of astroglia

Because of the intriguing signs of astrocytic degeneration and decay we wondered if this observation could be substantiated by quantitative data. Therefore, a limited morphometric analysis of the astrocytic cell population on the basis of GFAP immunostains was performed. The results of astroglia counts in CPM cases and normal controls are given in Table 3.

Compared with normal controls the average number of astrocytes in CPM cases was increased within the lesion as well as in lateral unaffected pontine tissue, e.g., lateral pontine tissue from CPM cases contained 28% more astrocytes ($P = 0.023$) than the equivalent tissue of control cases. Evaluation of quantitative data from distinct sectors of individual pontine sections led to conflicting results. In four CPM cases astrocytes were diminished within the lesion as compared to the adjacent non-demyelinated areas, although these results were not statistically significant ($P = 0.398$). Interestingly, all of these four cases revealed severe degenerative changes of the astrocytes as well as GFAP⁺ macrophages within the lesion. In the other three cases the number of astrocytes

was increased within the demyelinated foci. Here, numerous hypertrophic and multinucleated astrocytes with occasionally faint GFAP immunolabeling were prominent. In one of these latter cases (g) an astrocytic mitosis was found.

As was to be expected the number of astrocytes within central and lateral parts of the pons showed virtually no differences ($P = 0.144$) in normal control cases.

Discussion

Since the first description of CPM by Adams et al. in 1959 [2], nearly 500 cases of this demyelinating disease have been published. Evidence has recently been accumulated that implicates a role for electrolyte imbalances, in particular rapid rise in serum sodium, in contributing to CPM [21, 25, 37]. However, this is still hypothetical and its relevance for the pathogenesis of CPM remains to be ascertained. Immunohistochemical investigations which could help to shed some light on the pathogenic events of CPM have not been reported. Therefore, we carried out an immunohistochemical examination of ten CPM

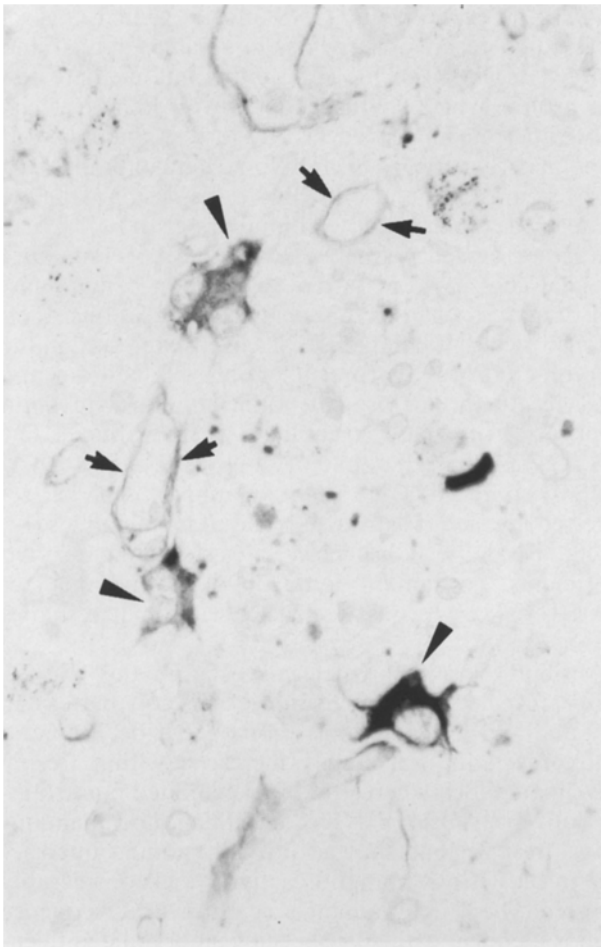


Fig. 8. Immunostaining of laminin in a case with fresh CPM (case 7; slight counterstaining with hemalum). In the center of the lesion three reactive astrocytes (*arrowheads*) show positive immunostaining. *Arrows* point to positively labeled basal laminas of blood vessels. Amplification of the peroxidase reaction product by silver intensification, $\times 580$

cases of differing histopathological age. As was to be expected, fresh and old lesions revealed severe degenerative alterations of oligodendrocytes and myelin sheaths which is reflected by altered immunostaining with MBP, MAG, transferrin and CA C antibodies. With the help of immunohistochemical methods, astrocytes were shown to display changes which consisted of intracytoplasmic vacuoles, shrunken perikarya with sparse processes, and lobulated or pyknotic nuclei.

Moreover, these severe astrocytic alterations obviously lead to cell death which can be assumed from the occurrence of GFAP⁺ macrophages. Macrophages are primarily GFAP⁻ cells, however they can take up GFAP⁺ material when astrocytes decay, e.g., in glioblastomas [9]. To test if the necrotic changes of astrocytes lead to a reduction of the astroglia in CPM foci, we decided to count this cell type in seven selected cases with fresh demyelination. Cases with old CPM foci were excluded because reactive fibrillary astrocytes can fail to react with anti-GFAP, presumably due to polymerization of the glial filaments which may reduce antigenically active sites [8, 10]. The results show that in four cases reduction of astroglia within the CPM lesions has occurred when compared with lateral unaffected pontine tissue. Simultaneously, astrocytes inside the foci exhibited degenerative alterations with the overall aspect of cell death. In the remaining three cases the number of astrocytes was increased within the lesions and here, in contrast to the above cases the astroglia most notably revealed properties of activation, such as hypertrophy, multinuclearity and faint GFAP immunolabeling, while necrotic alterations were infrequent. However, it is possible that these changes represent only a transient stage and may finally end up in necrosis.

In general, comparison of CPM cases with controls showed that in the former group the average number of astrocytes was increased within the lesion and in unaffected pontine tissue. Astrocyte proliferation in CPM has

Table 3. Density of astrocytes in seven cases of recent CPM and four control cases^a

CPM cases ($n = 7$) ^b			Control cases ($n = 4$)		
Case	Mean number of astrocytes/mm ²		Case	Mean number of astrocytes/mm ²	
	Central (lesion)	Lateral (unaffected)		Central	Lateral
a	50.71 (± 6.66)	95.49 (± 4.74)	h	53.56 (± 3.92)	52.80 (± 3.60)
b	56.87 (± 2.43)	93.91 (± 7.06)	i	61.04 (± 4.75)	61.11 (± 3.47)
c	70.52 (± 3.03)	91.98 (± 2.41)	j	86.11 (± 3.94)	83.07 (± 4.62)
d	90.65 (± 4.04)	95.57 (± 5.29)	k	54.95 (± 1.92)	53.68 (± 2.63)
e	61.01 (± 1.08)	57.79 (± 5.37)			
f	97.49 (± 4.23)	87.20 (± 1.71)			
g	115.92 (± 3.51)	83.53 (± 2.73)			
Mean ^c	$\bar{x}77.60 \pm 9.15$	$\bar{x}86.49^* \pm 5.82$		$\bar{x}63.91 \pm 7.58$	$\bar{x}62.67^* \pm 7.05$

^a Figures express mean number of four individual counts \pm SD

^b All CPM cases presented chronic alcoholism, with fatty liver changes in a, c, f, g and liver cirrhosis in d and e

^c Mean values of central and lateral portion of each group \pm SEM

* Significance at $P = 0.023$ when differences between lateral areas of CPM and control cases were assessed. Comparison between the remaining values revealed no statistical significance

been described by several authors [39, 46], probably due to primary underlying disorders, such as hepatic diseases. In our cases in which astroglial proliferation was found, clinical signs and histopathological evidence, i.e., Alzheimer type II glia for hepatic encephalopathy, were absent. In seven of our cases, we observed club- or rod-like, strongly GFAP⁺ structures which resembled Rosenthal fibers. The formation of Rosenthal fibers within CPM foci has also been reported by other authors [41, 56].

Our results unambiguously show that degenerative changes of astrocytes are a distinctive feature of CPM, but whether the abnormalities are of primary or secondary nature cannot be decided by histological inspection of autopsy cases. Several authors have discussed the potential pathogenic role of an impaired astroglial function in CPM [23, 36, 37]. It has been suggested that a rapid rise in serum sodium after sustained hyponatremia could be responsible for myelinolysis [21, 25, 37]. However, uncorrected chronic hyponatremia itself does not lead to demyelination, as was shown in an experimental model [21, 25] and in man [38], but causes ultrastructurally severe swelling of astrocytes and their processes [54]. Similar lesions could be observed in an experimental model of CPM [35] and in ultrastructural examination of human cases [42]. Goebel and Herman-Ben Zur [16] described abnormal impregnation of astrocytes with gold sublimate in some cases of CPM associated with electrolyte disturbances. From these results, taken together with our own report, it could be speculated that already pre-damaged astroglia (for instance, during ongoing liver disease) may be further damaged by severe electrolyte disturbances. Norenberg [36] has proposed a complex pathogenic model for CPM. A rapid rise in the serum sodium level may cause an osmotic injury to the endothelium resulting in the release of myelinotoxic factors and/or the production of vasogenic edema. An underlying gliopathy may potentiate the effect of osmotic stress by inappropriate compensation of hyperosmolarity.

In recent CPM lesions we observed weakly GFAP-labeled hypertrophic astrocytes. It is possible that the amount or the structure of this type of intermediate filaments may be altered as an effect of the demyelinating disease or due to underlying factors causing CPM. Faint labeling, or even a total lack of staining for GFAP, have previously been described for neoplastic astrocytes [10, 53]. Loss of GFAP immunoreactivity was also observed in Alzheimer type II glia. It has been suggested that this phenomenon is induced by uncontrolled calcium influx into astrocytes, causing proteolysis of GFAP [11]. At variance with other reports [16, 46], we did not see Alzheimer type II glia in our cases.

An alternative explanation for the weak GFAP staining in fresh CPM foci could be that reactive astrocytes regain an immature phenotype. This hypothesis is attractive since these glial cells simultaneously express vimentin. Immunocytochemical studies of CNS development have shown that early astrocytes are characterized by intermediate filaments containing vimentin, but not GFAP [7, 12]. Similar observations have been obtained from neoplastic astrocytes of experimentally induced gliomas

[43]. Also, in experimental CNS injuries, vimentin is re-expressed by reactive astrocytes in areas of axonal and nerve cell degeneration [6, 17]. Another intermediate filament protein which we investigated was desmin, which has been detected in astrocytes and Müller glia of the rat [5] and in early neurons of embryonic human brains [49]. However, in recent and old CPM cases desmin labeling was not detectable except for blood vessels.

Further evidence for the occurrence of immature astroglial cells in CPM is the observation of laminin⁺ reactive astrocytes in freshly demyelinated lesions. Liesi demonstrated that laminin is extensively expressed in the embryonic rat brain by precursors of both neurons and glial cells. In the mature rat brain, laminin expression disappears from these structures, except within a few CNS regions, e.g., the olfactory bulb [28]. After experimentally induced CNS injury laminin can be re-expressed in reactive astrocytes of adult mammals [14, 29, 48]. Recently, it has been suggested from *in vivo* experiments that laminin is not involved in axonal regrowth [14, 48], which is at variance with *in vitro* studies [24, 32].

Antibodies to the X-determinant and the HNK-1 epitope revealed a characteristic expression pattern in fresh and old CPM lesions. For the X-determinant, immunoreactivity was highly increased within freshly demyelinated foci, whereas old foci exhibited faint staining. Conversely, using HNK-1 specific monoclonal antibodies, fresh lesions showed normal staining intensity while in old lesions immunoreactivity was considerably enhanced. The X-determinant is a carbohydrate sequence which is identical with stage-specific embryonic antigen-1 (SSEA-1) that seems to act as an intercellular adhesion molecule in preimplantation embryos [47]. Recently it was shown that the X-determinant is expressed during prenatal stages of CNS development [45] and is involved in oligodendrocyte-astrocyte and astrocyte-astrocyte adhesion *in vitro* [34]. Therefore, it seems very likely that the X-determinant also functions as cell adhesion molecule of mature CNS tissue.

Taken together our results show that in CPM, besides destruction of oligodendroglia and myelin, dystrophy of the astroglia may also occur. The latter could be of pathogenic relevance in the demyelinating disease. The observation of increased X-hapten immunoreactivity in astroglia corroborates our detection of re-expression of vimentin and laminin which could mean that mature astroglia may revert back to an immature form. This reversion might be induced by microenvironmental influences generated by the mechanisms which have been suggested by Norenberg [36] (see above). We speculate that the re-activation of glial differentiation phenomena represents a transient cellular stress reaction which eventually may end up either in cell death or formation of typical gliosis.

Acknowledgements. The excellent technical assistance of K. Heigl is gratefully acknowledged. We thank Dr. T. Kumpulainen for the kind gift of CA C antibody and Dr. F. Kirchhoff for a sample of MAG antibody. The authors wish to thank Prof. Dr. J. Berger (Institut für Mathematik und Datenverarbeitung in der Medizin, Universität Hamburg) for performing statistical analysis. We are

also gratefully indebted to Dr. R. Laas (Abteilung für Neuropathologie und experimentelle Hirnforschung, Universität Hamburg) for providing us with autopsy material of CPM.

References

- Abo T, Balch CM (1981) A differentiation antigen of human NK and K cells identified by a monoclonal antibody (HNK-1). *J Immunol* 127:1024–1029
- Adams RD, Victor M, Mancall EL (1959) Central pontine myelinolysis. A hitherto undescribed disease occurring in alcoholic and malnourished patients. *Arch Neurol Psychiatry* 81:154–172
- Bartsch U, Kirchhoff F, Schachner M (1989) Immunohistological localization of the adhesion molecules L1, N-CAM, and MAG in the developing and adult optic nerve of mice. *J Comp Neurol* 284:451–462
- Bloch B, Popovici T, Levin MJ, Tuil D, Kahn A (1985) Transferin gene expression visualized in oligodendrocytes of the rat brain by using in situ hybridization and immunohistochemistry. *Proc Natl Acad Sci USA* 82:6706–6710
- Dahl D, Bignami A (1982) Immunohistological localization of desmin, the muscle-type 100 Å filament protein, in rat astrocytes and Müller glia. *J Histochem Cytochem* 30:207–213
- Dahl D, Bignami A, Weber K, Osborn M (1981) Filament proteins in rat optic nerves undergoing Wallerian degeneration. Localization of vimentin, the fibroblastic 100-Å filament protein, in normal and reactive astrocytes. *Exp Neurol* 73:496–506
- Dahl D, Rueger DC, Bignami A, Weber K, Osborn M (1981) Vimentin, the 57000 molecular weight protein of fibroblast filaments, is the major cytoskeletal component in immature glia. *Eur J Cell Biol* 24:191–196
- DeArmond SJ, Eng LF, Rubinstein LJ (1980) The application of glial fibrillary acidic (GFA) protein immunohistochemistry in neurooncology. A progress report. *Pathol Res Pract* 168:374–394
- Deck JHN, Rubinstein LJ (1981) Glial fibrillary acidic protein in stromal cells of some capillary hemangioblastomas. Significance and possible implications of an immunoperoxidase study. *Acta Neuropathol (Berl)* 54:173–181
- Eng LF, DeArmond SJ (1982) Immunocytochemical studies of astrocytes in normal development and disease. In: Fedoroff S, Hertz L (eds) *Advances in cellular neurobiology*, vol 3. Academic Press, London, pp 145–171
- Eng LF, DeArmond SJ (1983) Immunocytochemistry of the glial fibrillary acidic protein. In: Zimmermann HM (ed) *Progress in neuropathology*, vol 5. Raven Press, New York, pp 19–39
- Fedoroff S, White RV, Neal J, Subrahmanyam L, Kalnins VI (1983) Astrocyte cell lineage. II. Mouse fibrous astrocytes and reactive astrocytes in cultures have vimentin- and GFP-containing intermediate filaments. *Dev Brain Res* 7:303–315
- Gallyas F, Merenthaler I (1988) Copper-H₂O₂ oxidation strikingly improves silver intensification of the nickel-diaminobenzidine (Ni-DAB) end-product of the peroxidase reaction. *J Histochem Cytochem* 36:807–810
- Giftchristos N, David S (1988) Laminin and heparan sulphate proteoglycan in the lesioned adult mammalian central nervous system and their possible relationship to axonal sprouting. *J Neurocytol* 17:385–397
- Gocht A, Colmant HJ (1987) Central pontine and extrapontine myelinolysis. A report of 58 cases. *Clin Neuropathol* 6:262–270
- Goebel HH, Herman-Ben Zur P (1976) Central pontine myelinolysis. *Handb Clin Neurol* 28:285–316
- Graeber MB, Streit WJ, Kreutzberg GW (1989) Formation of microglia-derived brain macrophages is blocked by adriamycin. *Acta Neuropathol* 78:348–358
- Graham RC, Karnovsky MJ (1966) The early stages of absorption of injected horseradish peroxidase in the proximal tubules of mouse kidney. Ultrastructural cytochemistry by a new technique. *J Histochem Cytochem* 14:291–301
- Hanjan SNS, Kearney JF, Cooper MD (1982) A monoclonal antibody (MMA) that identifies a differentiation antigen on human myelomonocytic cells. *Clin Immunol Immunopathol* 23:172–188
- Hsu SM, Raine L, Fanger H (1981) Use of avidin-biotin-peroxidase complex (ABC) in immunoperoxidase techniques. A comparison between ABC and unlabeled antibody (PAP) procedures. *J Histochem Cytochem* 9:577–580
- Illowsky B, Laureno R (1987) Encephalopathy and myelinolysis after rapid correction of hyponatraemia. *Brain* 110:855–867
- Itoyama Y, Sternberger NH, Kies MW, Cohen SR, Richardson EP, Webster HdeF (1980) Immunocytochemical method to identify myelin basic protein in oligodendroglia and myelin sheaths of the human nervous system. *Ann Neurol* 7:157–166
- Jellinger K (1968) Zur Neuropathologie des Komats und postkomatöser Encephalopathien. *Wien klin Wochenschr* 80:505–517
- Kleinman HK, Ogle RC, Cannon FB, Little CD, Sweeney TM, Luckenbill-Edds L (1988) Laminin receptors for neurite formation. *Proc Natl Acad Sci USA* 85:1281–1286
- Kleinschmidt-DeMasters BK, Norenberg MD (1981) Rapid correction of hyponatremia causes demyelination. Relation to central pontine myelinolysis. *Science* 211:1068–1070
- Kumpulainen T, Korhonen LK (1982) Immunohistochemical localization of carbonic anhydrase isoenzyme C in the central and peripheral nervous system of the mouse. *J Histochem Cytochem* 30:283–292
- Kumpulainen T, Nyström SHM (1981) Immunohistochemical localization of carbonic anhydrase isoenzyme C in human brain. *Brain Res* 220:220–225
- Liesi P (1985) Do neurons in the vertebrate CNS migrate on laminin? *EMBO J* 4:1163–1170
- Liesi P, Kaakkola S, Dahl D, Vaheri A (1984) Laminin is induced by astrocytes of adult brain by injury. *EMBO J* 3:683–686
- Ludwin SK, Kosek JC, Eng LF (1976) The topographical distribution of S-100 and GFA proteins in the adult rat brain. An immunohistochemical study using horseradish peroxidase-labelled antibodies. *J Comp Neurol* 165:197–208
- Mai JK, Reifenberger G (1988) Distribution of the carbohydrate epitope 3-fucosyl-N-acetyllactosamine (FAL) in the adult human brain. *J Chem Neuroanat* 1:255–285
- Manthorpe M, Engvall E, Ruoslahti E, Longo FM, Davis GE, Varon S (1983) Laminin promotes neurite regeneration from cultured peripheral and central neurons. *J Cell Biol* 97:1882–1890
- Mason DY, Woolston R-E (1982) Double immunoenzymatic labelling. In: Bullock GR, Petrusz P (eds) *Techniques in immunocytochemistry*, vol 1. Academic Press, London, pp 135–153
- Niedieck B, Löhler J (1987) Expression of 3-fucosyl-N-acetyllactosamine on glia cells and its putative role in cell adhesion. *Acta Neuropathol (Berl)* 75:173–184
- Norenberg MD (1981) Ultrastructural observations in electrolyte-induced myelinolysis (abstract). *J Neuropathol Exp Neurol* 40:319
- Norenberg MD (1983) A hypothesis of osmotic endothelial injury. A pathogenetic mechanism in central pontine myelinolysis. *Arch Neurol* 40:66–69
- Norenberg MD, Papendick RE (1984) Chronicity of hyponatremia as a factor in experimental myelinolysis. *Ann Neurol* 15:544–547
- Norenberg MD, Leslie KO, Robertson AS (1982) Association between rise in serum sodium and central pontine myelinolysis. *Ann Neurol* 11:128–135
- Okeda R, Kitano M, Sawabe M, Yamada I, Yamada M (1986) Distribution of demyelinating lesions in pontine and extrapont-

- tine myelinolysis. Three autopsy cases including one case devoid of central pontine myelinolysis. *Acta Neuropathol (Berl)* 69:259–266
40. Perentes E, Rubinstein LJ (1985) Immunohistochemical recognition of human nerve sheath tumors by anti-Leu 7 (HNK-1) monoclonal antibody. *Acta Neuropathol (Berl)* 68:319–324
 41. Pogacar S (1980) Iatrogenic precipitation of central pontine myelinolysis with formation of Rosenthal fibers (abstract). *J Neuropathol Exp Neurol* 39:383
 42. Powers JM, McKeever PE (1976) Central pontine myelinolysis. An ultrastructural and elemental study. *J Neurol Sci* 29:65–81
 43. Reifenberger G, Bilzer T, Seitz RJ, Wechsler W (1989) Expression of vimentin and glial fibrillary acidic protein in ethylnitrosourea-induced rat gliomas and glioma cell lines. *Acta Neuropathol* 78:270–282
 44. Rutishauser U, Jessell TM (1988) Cell adhesion molecules in vertebrate neural development. *Physiol Rev* 68:819–857
 45. Schwarting GA, Yamamoto M (1988) Expression of glycoconjugates during development of the vertebrate nervous system. *Bio Essay* 9:19–23
 46. Seitelberger F (1973) Zentrale pontine Myelinolyse. *Schweiz Arch Neurol Neurochir Psychiatr* 112:285–297
 47. Solter D, Knowles BB (1978) Monoclonal antibody defining a stage-specific mouse embryonic antigen (SSEA-1). *Proc Natl Acad Sci USA* 75:5565–5569
 48. Sosale A, Robson JA, Stelzner DJ (1988) Laminin distribution during corticospinal tract development and after spinal cord injury. *Exp Neurol* 102:14–22
 49. Stagaard M, Møllgård K (1989) The developing neuroepithelium in human embryonic and fetal brain studied with vimentin-immunocytochemistry. *Anat Embryol* 180:17–28
 50. Sternberger LA (1986) *Immunocytochemistry*, 3rd edn. Wiley, New York
 51. Sternberger NH, Quarles RH, Itoyama Y, Webster HdeF (1979) Myelin-associated glycoprotein demonstrated immunocytochemically in myelin and myelin-forming cells of developing rat. *Proc Natl Acad Sci USA* 76:1510–1514
 52. Timpl R, Rhode H, Robey PG, Rennard SI, Foidart J-M, Martin GR (1979) Laminin. A glycoprotein from basement membranes. *J Biol Chem* 254:9933–9937
 53. Van der Meulen JDM, Houthoff HJ, Ebels EJ (1978) Glial fibrillary acidic protein in human gliomas. *Neuropathol Appl Neurobiol* 4:177–190
 54. Wasterlain CG, Torack RM (1968) Cerebral edema in water intoxication. II. An ultrastructural study. *Arch Neurol* 19:79–87
 55. Weibel ER (1979) *Stereological methods. Practical methods for biological morphometry*, vol 1. Academic Press, London
 56. Wildi E (1973) Contribution à l'anatomo-clinique de la myélinolyse du pont. *Schweiz Arch Neurol Neurochir Psychiatr* 112:271–284
 57. Wright DG, Lauren R, Victor M (1979) Pontine and extrapontine myelinolysis. *Brain* 102:361–385